IRIS AperTO

UNIVERSITÀ DEGLI STUDI DI TORINO

AperTO - Archivio Istituzionale Open Access dell'Università di Torino

Adsorption of acid dyes on fungal biomass: Equilibrium and kinetics characterization

This is the author's manuscript

Original Citation:

Availability:

This version is available http://hdl.handle.net/2318/74535 since 2016-10-04T17:06:14Z

Published version:

DOI:10.1016/j.cej.2010.05.058

Terms of use:

Open Access

Anyone can freely access the full text of works made available as "Open Access". Works made available under a Creative Commons license can be used according to the terms and conditions of said license. Use of all other works requires consent of the right holder (author or publisher) if not exempted from copyright protection by the applicable law.

(Article begins on next page)

08 November 2026

IRIS AperTO

UNIVERSITÀ DEGLI STUDI DI TORINO

This Accepted Author Manuscript (AAM) is copyrighted and published by Elsevier. It is posted here by agreement between Elsevier and the University of Turin. Changes resulting from the publishing process - such as editing, corrections, structural formatting, and other quality control mechanisms - may not be reflected in this version of the text. The definitive version of the text was subsequently published in CHEMICAL ENGINEERING JOURNAL, 162(2), 2010, 10.1016/j.cej.2010.05.058.

You may download, copy and otherwise use the AAM for non-commercial purposes provided that your license is limited by the following restrictions:

(1) You may use this AAM for non-commercial purposes only under the terms of the CC-BY-NC-ND license.

(2) The integrity of the work and identification of the author, copyright owner, and publisher must be preserved in any copy.

(3) You must attribute this AAM in the following format: Creative Commons BY-NC-ND license (http://creativecommons.org/licenses/by-nc-nd/4.0/deed.en), 10.1016/j.cej.2010.05.058

The publisher's version is available at:
http://linkinghub.elsevier.com/retrieve/pii/S1385894710005139

When citing, please refer to the published version.

Link to this full text:
http://hdl.handle.net/2318/74535

This full text was downloaded from iris - AperTO: https://iris.unito.it/

iris - AperTO

University of Turin's Institutional Research Information System and Open Access Institutional Repository

Adsorption of acid dyes on fungal biomass: Equilibrium and kinetics characterization

M.E. Russo[a], F. Di Natale[a], V. Prigione[b], V. Tigini[b], A. Marzocchella[a,], G.C. Varese[b]

[a] Dipartimento di Ingegneria Chimica, Università degli Studi di Napoli Federico II, P.le V. Tecchio n. 80, 80125 Napoli, Italy

[b] Dipartimento di Biologia Vegetale, Università degli Studi di Torino, Viale Mattioli n. 25, 10125 Torino, Italy

Abstract

Dyes adsorption on granular particles of lyophilised *Cunninghamella elegans* was characterized in terms of adsorption isotherm and kinetics. The study refers to dyes of an acid bath for wool: Acid Blue 62, Acid Red 266 and Acid Yellow 49. The dye concentration in model solutions – containing a single dye or the three dyes all together in order to mimic the wastewater – was increased up to about 500 mg/L. Tests showed that the maximum adsorption capacity of the biomass ranges between 300 and 600 mg_{dye}/g_{DM}. Mutual interferences among dyes caused the reduction of the adsorption capacity of the biomass towards the model wastewater. An experimental procedure for the assessment of biosorption kinetics was developed in order to control the effects of the interphase mass transfer on the biosorption rate. The biosorption kinetics were described by both pseudo-first order and pseudo-second order models, depending on the saturation level of the sorbent, and was characterized by a time scale of 1–10 min. The role of the molecular structures of the dyes was discussed. In particular, both kinetics and equilibrium tests confirm that the biomass is more selective towards AR266, probably for the high negative charge density of the $–CF_3$ functional group that can interact with $–NH_x$ active sites of the biomass.

Keywords

- Biosorption;
- Acid dyes;
- Kinetics;
- Fungal biomass

Nomenclature

A particle surface per unit volume of particle, 1/m

C dye concentration in liquid phase, mg/L

$\langle c \rangle$ average dye concentration in the liquid across the packed bed, mg/L

c_T dye concentration in the liquid in the tank, mg/L

c_T^0 dye concentration in the liquid in the tank at $t = 0$, mg/L

F liquid flow rate, mL/min

K mass transfer rate, 1/s

k_1 kinetic constant, 1/min

k_2 kinetic constant, g/(mg min)

K_F Freundlich constant $(mg^{(n-1)}\ L)^{1/n}/g$

K_L pseudo-equilibrium constant, L/g

M mass of biosorbent, g

n Freundlich exponent

q adsorbed dye concentration, mg/g

$\langle q \rangle$ average adsorbed dye concentration on the biomass packed bed, mg/L

Q_{max} maximum adsorption capacity, mg/g

r_{ads} adsorption rate, mg/(g min)

t time, min

V_B liquid volume in the packed bed, mL

V_T liquid volume in the tank, mL

Subscripts

s value at the liquid–solid interface

eq value approaching equilibrium

1 referred to pseudo-first order kinetic model

2 referred to pseudo-second order kinetic model

ref referred to reference concentration of dye in treated wastewater

Greek

λ_{max} wavelength of maximum absorbance, nm

ε extinction coefficient, L/(mg cm)

ϑ critical value of the ratio between adsorbed dye concentration and its equilibrium value

1. Introduction

Wastewaters polluted by dyes represent a relevant issue associated with several industries. Dyes, even at low concentrations, reduce wastewater transparency and oxygen solubility and are often toxic and mutagenic for the aquatic flora and fauna [1].

Both the aerobic and anaerobic bioremediation processes are usually hindered by the harsh environment (salt concentration, pH…) that may inhibit the biological activity of the microorganisms, while physical and chemical treatments of coloured wastewaters are often technically or economically unfeasible [2] and [3]. In addition, the wide fluctuations of composition, pH and temperature of the coloured water streams make the treatment processes still more difficult to design and to control [3]. Chemical and physical treatments adopted have been reviewed by Robinson et al. [4]. They pointed out that the main disadvantage related with chemical methods (as Fenton reagents oxidation, ozonations, photochemical degradations and sodium hypoclorite addition) is the formation of toxic compounds resulting from the cleavage of the chromophoric groups. The same phenomenon may also affect the anaerobic bioremediation of dye-containing wastewaters [5].

Adsorption is one of the most reliable and versatile physical treatments whose effectiveness and economic sustainability is strictly related to the type of sorbent. The activated carbons are the most largely adopted sorbents for the removal of pollutants from water effluents because they are characterized by high uptake capacity towards different class of substances – from metallic ions to organic compounds – and by satisfactory mechanical properties that allow their use in industrial equipments. The main disadvantages of activated carbons are the unit cost of the virgin material (about 1 US dollar/kg) and the absence of reliable methods for sorbent regeneration (thermal regeneration costs are about 1–2 US dollar/kg).

In the last twenty years, studies concerning the adsorption on biomass (biosorption) have highlighted its potentiality as a suitable method for water remediation. Biosorption is defined as the passive uptake of organic or inorganic species from aqueous solutions by microbial biomasses (bacteria, yeasts, filamentous fungi and algae) or waste materials from industry and agriculture (i.e. pinewood, corncob, bagasse, rice husk, chitosan, etc.). The process encompasses a number of metabolism-independent phenomena (physical and chemical adsorptions, electrostatic interaction, ion exchange, complexation, chelation and micro precipitation) that mainly take place at the cell wall level [6].

The dye adsorption on biomass provides two main advantages: (i) biomass is a quite unexpensive sorbent, often recovered as waste material, and the spent sorbent may be digested through solid state fermentations [4]; (ii) the composition of the cell wall and the inactivation procedure (cell disruption through autoclaving) provide wide diversity of the active sites and large specific surface. The latter feature enhances the decolourization process of textile effluents, that usually contain several dyes, each of which characterized by different functional groups. Only few studies on the biosorption rates and uptake capacities in model solutions containing multiple dyes – to emulate realistic industrial effluents – are available in the literature [7], [8], [9], [10] and [11], and the mechanisms responsible for the biosorption of dyes are still under investigation.

Even though the elective technology for the adsorption processes is the fixed bed, biomasses are often not appropriate for these apparatus as a consequence of their low mechanical stress resistance, high compressibility, and their tendency to swell in water. A possible strategy to overcome this issue is the biomass immobilization, but the process becomes definitively very expensive [6]. On

the other hand, technologies based on suspended biomass may be successful but information available in the literature to support scale-up is still lacking.

The interest in the elucidation of biosorption mechanisms drives the research towards the selection of proper models to describe both biosorption kinetics and thermodynamics. This characterization becomes more urgent whether the design and the optimization of industrial adsorbing units are required. For these reasons, the experimental investigations on batch or continuous biosorption of dyes and metals are often enriched by the analysis of experimental data with the most common empirical and theoretical models [12], [13] and [14]. The thermodynamic behaviour of dye solution/biomass systems is mainly investigated by the well known Langmuir and Freundlich models.

A hindrance to the dye biosorption modelling is posed by the impurities content of the commercially available dyestuff powders. In fact, the presence of unknown quantities of additives and salts does not allow to study the biosorption on molar basis of the chromophoric compound alone.

The kinetics of dye biosorption is often described by applying the Lagergren pseudo-first order model and the Ho and McKay pseudo-second order model. The first is valid for far-from-saturation conditions, i.e. at the early stage of biosorption on virgin biomass. The pseudo-second order kinetic model can be successfully adopted to describe the biosorption process over a wider time interval, also close to the equilibrium conditions.

The reported scenario suggests that the development of novel biomasses having high adsorption capacity towards specific pollutants asks for the characterization of biosorption equilibrium and kinetics. Recent studies have shown that inactivated biomass of the zygomycetes *Cunninghamella elegans* proven to be a reliable and cost effective alternative to activated carbon to remove dyes and chromium from water [10], [11] and [15].

The present work moves one step further along the direction of characterizing the biosorption equilibrium and kinetics of *C. elegans* towards acid dyes. The investigation has been carried out with the aim to assess:

- The biomass equilibrium adsorption capacity in model wastewater containing one or more acid dyes.
- The intrinsic biosorption rates adopting experimental procedures characterized by negligible external mass transport resistance.

The attention has been focused on the acid dye components of a bath for wool identified as a model wastewater (MW) within the EC FP6 Project SOPHIED [11]. In particular, Acid Blue 62 (ABu62), Acid Red 266 (AR266), and Acid Yellow 49 (AY49) were investigated as single-dye solutions and as MW. The investigation was carried out in a lab-scale fixed bed device purposely designed to control the mass transfer rates during the adsorption kinetics tests. The experimental results were analysed in the light of the Lagergren and the Ho-McKay pseudo-second order models to estimate the kinetic parameters related to the biosorption of both single dyes and MW.

2. Materials and methods

2.1. Dyes

Three acid dyes adopted in dye baths for wool [11] were investigated (Fig. 1): Acid Blue 62 (ABu62), Acid Red 266 (AR266), Acid Yellow 49 (AY49). The purity of the dyes (Town End, Leeds, UK) ranged between 50 and 90 wt.%. Tests were also carried out with solutions of the three dyes to mimic a real wastewater: mass ratio among the three dyes was fixed at 1:1:1.

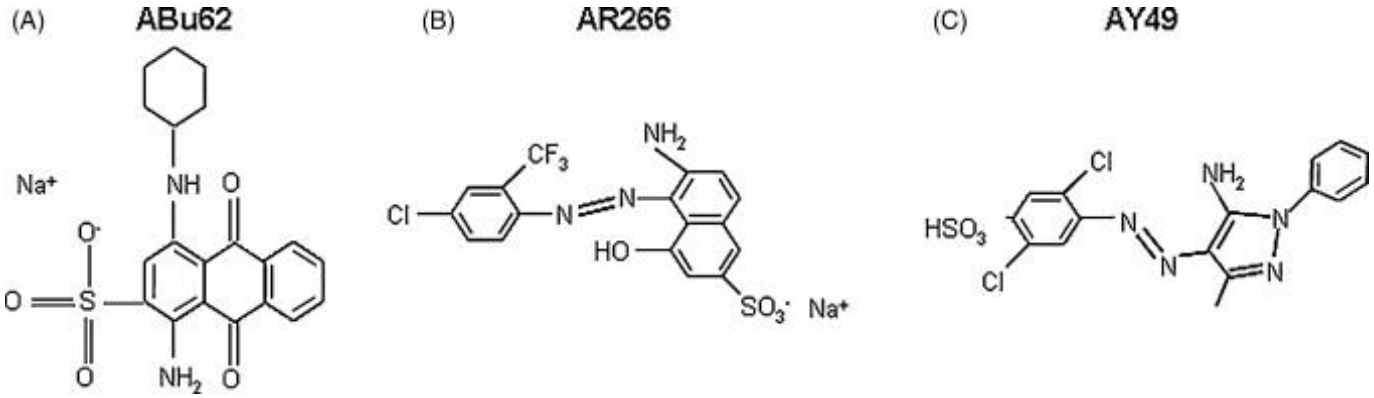

Fig. 1. Chemical structures of acid dyes: (A) ABu62, (B) AR266 and (C) AY49.

Dyes were dissolved in 2 g/L Na_2SO_4 solution. The initial concentration of the dye in the mono-component solutions ranged between 50 and 500 mg/L, and the initial overall concentration in the MW ranged between 60 and 300 mg/L.

The initial pH of the solutions and of the MW was fixed at 5 by adding acetic acid according to Prigione et al. [11]

2.2. Biosorbent

C. elegans Lendner (MUT 2861) was obtained from the *Mycotheca Universitatis Taurinensis* Collection (MUT, University of Turin, Department of Plant Biology). It was patented for dye biosorption [16] and deposited at the Deutsche Sammlung von Mikroorganismen und Zellkulturen (DSMZ-Braunschweig, Germany). Starting cultures of this fungus were lyophilised and cryopreserved until use. They were revitalised on MEA and mature conidia for the inocula and biomass production were obtained from cultures grown on the same medium in the dark at 24 °C for 1 week.

C. elegans was cultured as described by Prigione et al. [15], harvested, autoclaved (30 min at 121 °C) and lyophilised (Lyophiliser LIO 10P, Cinquepascal, Trezzano s/n, Italy). The lyophilised biomass was sieved in the range 300–600 μm.

2.3. Dye concentration measurement

Dye concentration was measured as optical absorbance of the solutions by means of a spectrophotometer (Cary 50, Varian Inc.). The maximum absorption wavelengths (λ_{max}) for the single dye were: 595 and 636 nm for ABu62; 495 nm for AR266; 401 nm for AY49. The concentration of the ABu62 was estimated as optical absorbance at λ_{max} = 636 nm, being the two main peaks of the spectrum almost equivalent. Calibration tests were carried out to assess the extinction coefficient of each dye (ε_i).

The spectrum of the MW was compared with those of the single dyes to analyse possible mutual interference. The absorbance at the selected λ_{max} of the three dyes was measured and compared with the expected value, calculated by means of the ε_i and the concentration. The deviation of the measured value with respect to the expected value was adopted to assess the extinction coefficient for the three dyes in the MW.

The calibration procedure was carried out both in a 1 mm quartz flow cell (Starna Scientific Limited, UK) and in plastic disposable cuvette (Kartell®).

2.4. Apparatus

The apparatus adopted for the characterization of the biosorption kinetics consisted of a bioadsorption column, a buffer tank, a gear pump (VG 1000 digit, Verder), and an on-line flow cell. The column (8 mm I.D., and 60 mm high) was made of Plexiglas and was equipped with stainless steel nets at both end sections to prevent solids entrainment. The biomass loaded in the column was mixed with 300 μm glass beads, to prevent bed clogging and to evenly distribute liquid flow across the bed. The on-line flow cell housed in the spectrophotometer allowed the continuous measurement (sampling frequency about 0.2 Hz) of the optical absorbance of the liquid phase. The gear pump provided the continuous circulation of the dye solution between the buffer tank and the bioadsorption column under controlled volumetric flow rate conditions.

The mass of biosorbent loaded in the column ranged between 0.03 and 0.10 g. The solution volume in the buffer tank ranged between 0.1 and 0.2 L.

The equilibrium dye partition between the biosorbent and the liquid phase was investigated batchwise. Solids agitation during tests was accomplished by a rotary shaker set at 110 rpm.

Light-catalysed oxidation of the dye was prevented by wrapping vessels and pipes with aluminium foil.

Tests were carried out at 25 °C.

2.5. Experimental procedure and data analysis

2.5.1. Assessment of equilibrium conditions

Prefixed masses of sorbent (M) and volumes of dye solution (V) were mixed and kept in agitation on an orbital shaker for about 1 day. The solution was periodically sampled. Each sample was centrifuged for 5 min at 14,000 rpm and the dye concentration (c) in the recovered supernatant was measured. The dye uptake per unit mass of biomass at equilibrium (q) was determined by the mass balance:

equation(1)

$$Mq=V(c_0-c)Mq=V(c0-c)$$

where c_0 is the initial dye concentration in the liquid phase.

During tests with MW, the concentration of each dye in the liquid was measured and the associated dye uptake on the sorbent was calculated according to Eq. (1). Each test was carried out in triplicate.

Some tests were carried out to assess: (i) the role the spontaneous decoulorization of the solutions (e.g. degradation, photobleaching or complexation); (ii) the release of coloured species from the biomass. Accordingly, tests were carried out either with biomass mixed with dye-less aqueous solution or with mono-dye solutions without biomass. Within the instrumental accuracy, any alteration of the colour intensity was observed during the tests. Therefore, the reduction of colour intensity during the kinetics and equilibrium experiments can be ascribed only to the occurrence of biosorption phenomena.

2.5.2. Assessment of biosorption kinetics

The biosorption kinetic was assessed by working out the time-resolved measurements of the dye concentration in the apparatus described in Section 2.4. The procedure is based on the following steps: (i) the biomass was loaded in the adsorption unit and a set volume of dye solution was loaded in a well mixed buffer tank; (ii) the liquid started to circulate in the loop at the preset flow rate (F); (iii) the optical absorbance of the solution in the buffer tank was measured on-line until a constant value was approached; (iv) the time-series of the dye concentration in the mixed tank (c_T, t) was calculated by means of the appropriate extinction coefficient.

The biosorption rate was calculated by means of the mass balance on the dye. The following conditions were assumed:

(a)perfect mixing of the liquid phase in the buffer tank (volume V_T);

(b)the fixed bed adsorption unit is operated as a plug flow device characterized by low dye depletion. Accordingly, a small but finite concentration gradient establishes along the adsorption bed. Therefore, the behaviour of the unit is described by means of average instantaneous values of dye concentration in the liquid phase, $\langle c \rangle$, and in the biomass phase, $\langle q \rangle$;

(c)dye depletion rate in the liquid phase is controlled by the intraparticle adsorption kinetics, including intraparticle mass transfer phenomena and superficial reaction;

(d)the adopted apparatus is a closed system, the dye distributes between the liquid and solid phase.

The hypothesis (c) deserves some details. An intraparticle adsorption controlled regime establishes if the dye uptake rate (r_{ads}) at the biomass surface is smaller than the mass transfer rate across the boundary layer in the liquid phase around the particle:

equation(2)

$r_{ads} << ka(c - c_s)$rads<<ka(c−cs)

where k is the mass transfer coefficient in the boundary layer around a spherical particle of biosorbent, a the particle surface per unit volume of particle, c and c_s the dye concentrations in the liquid bulk and at the particle–liquid interface, respectively. The criterion Eq. (2) was verified comparing the characteristic time scale of mass transfer across the boundary layer with the time scale of the dye adsorption dynamics. In this study, the interphase mass transfer coefficient k was calculated according to the equations of Wilson and Geankoplis [17] and Kataoka et al. [18]. Provided that the time scale of the adsorption process is of the order of magnitude of minute, according to the adopted models [17] and [18] a liquid flow rate (F = 10 mL/min) verifies Eq. (2). Therefore, this flow rate was adopted for all the experimental campaign.

The mass balance on the dye extended to the volume of liquid (V_B) in the fixed bed reads:

equation(3)

$$M\frac{\mathrm{d}\langle q\rangle}{\mathrm{d}t} = -V_B\frac{\mathrm{d}\langle c\rangle}{\mathrm{d}t}$$ Md ⟨q⟩ dt=−VBd ⟨c⟩ dt

where M is the mass of biosorbent, $\langle q\rangle$ and $\langle c\rangle$ are the average volumetric concentrations of dye in the biomass and in the liquid, respectively.

The mass balance on the dye extended to the liquid phase in the buffer tank (V_T) reads:

equation(4)

$$V_T\frac{\mathrm{d}c_T}{\mathrm{d}t} = F(c_b - c_T)$$ VTdcTdt=F(cb−cT)

where c_b is the dye concentration in the outlet stream of the adsorption bed.

As a consequence of the assumption (d) it results:

equation(5)

$$V_B\frac{\mathrm{d}\langle c\rangle}{\mathrm{d}t} = V_T\frac{\mathrm{d}c_T}{\mathrm{d}t}$$ VBd ⟨c⟩ dt=VTdcTdt

Working out Eqs. (3) and (5) it results:

equation(6)

$$M\frac{\mathrm{d}\langle q\rangle}{\mathrm{d}t} = -V_T\frac{\mathrm{d}c_T}{\mathrm{d}t}$$ Md ⟨q⟩ dt=−VTdcTdt

At any instant, the accumulation of adsorbed dye in the packed bed is equal to the depletion of the dye in the buffer tank. Said c_T^0 cT0 the dye concentration in the liquid phase at the beginning of the test, the time-resolved concentration $\langle q\rangle$ may be calculated as a function of the dye concentration in the buffer tank c_T.

equation(7)

$$\langle q\rangle(t) = \frac{V_T}{M}(c_T^0 - c_T(t))$$ ⟨q⟩ (t)=VTM(cT0−cT(t))

3. Theoretical framework

3.1. Kinetics

The dye adsorption rate on biomass was assessed by means of a rate equation on dye assuming: (i) uniform mixed unit operated batchwise; (ii) negligible contribution of external mass transfer:

equation(8)

$$\frac{dq}{dt} = r_{ads}(q, q_{eq})$$ dqdt=rads(q,qeq)

where r_{ads} is the adsorption rate of the dye depending on the instantaneous dye concentration (q) and the dye equilibrium concentration (q_{eq}). For fresh biomass the initial condition is:

equation(9)

q(t=0)=0q(t=0)=0

In the present study, the dye sorption kinetics has been investigated with reference to relevant models available in the literature. In particular, the Lagergren kinetic model of pseudo-first order (Eq. (10)) and the kinetic model of pseudo-second order (Eq. (11)) [19] have been adopted:

equation(10)

$r_{ads}(q,q_{eq})=k_1(q_{eq}-q)$rads(q,qeq)=k1(qeq−q)

equation(11)

$r_{ads}(q,q_{eq})=k_2(q_{eq}-q)^2$rads(q,qeq)=k2(qeq−q)2

The system of Eqs. (8) and (9) has been integrated adopting both models Eqs. (10) and (11) and the linearization yields:

equation(12)

1st order kinetic $\ln(q_{eq}-q)=-k_1t+\ln(q_{eq})$1st order kinetic ln(qeq−q)=−k1t+ln(qeq)

equation(13)

2nd order kinetic $\frac{t}{q} = \frac{t}{q_{eq}} + \frac{1}{k_2 q_{eq}^2}$ 2nd order kinetic tq=tqeq+1k2qeq2

The parameters k_1 and k_2 were assessed by the numerical regression of the time-resolved measurements of $\langle q \rangle$ in agreement with Eqs. (12) and (13). The value of q_{eq} in Eq. (12) was estimated by means of Eq. (7) by setting $c_T = c_{Teq}$, the concentration measured at the end of tests.

3.2. Equilibrium

Experimental data have been worked out in agreement with the following models:

Langmuir model:

equation(14)

$$q = \frac{Q_{max} K_L c}{1 + K_L c}$$ q=QmaxKLc1+KLc

Linear isotherm:

equation(15)

q=K cq=K c

Freundlich model:

equation(16)

$q=K_F c1/nq=KFc1/n$

4. Results and discussion

4.1. Assessment of dyes biosorption kinetics

The kinetics of acid dyes biosorption on lyophilised biomass of *C. elegans* was extensively investigated following the procedures reported in Sections 2.5.2 and 3.1. Relevant results regarding the kinetics of biosorption of single dye and that of simultaneous biosorption of three dyes are detailed thereafter.

Fig. 2 shows the typical time-series of the adsorbed dye concentration $\langle q \rangle$ assessed by working out the data measured during the biosorption tests. The data refer to a test carried out with a solution of AR266 (initial concentration c_T^0 = 250 mg/L), at circulation liquid rate of 10 mL/min. The optical absorbance was on-line measured until it approached a steady state value. Remarkably, 90% of the equilibrium conditions established within about 25 min.

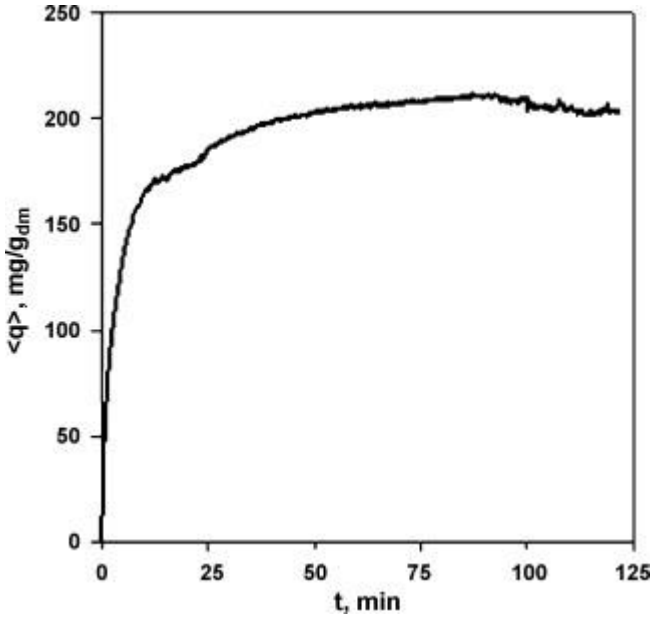

Fig. 2. Time-resolved concentration of adsorbed AR266 on *C. elegans*. Liquid volume: 0.2 L; biomass: 0.03 g; c_T^0 = 250 mg/L.

The assumption (c) reported in Section 2.5.2 can be verified working out the reported results. The characteristic time scale assessed for the mass transfer in the packed bed (1/*ka*) ranged between 0.7 and 1.3 s, resulting orders of magnitude smaller than the time scale of the observed adsorption rate. This favourable condition was verified for all the tests carried out in the experimental campaign.

The time-series of $\langle q \rangle$ obtained by means of Eq. (7) were worked out in agreement with Eqs. (12) and (13) to assess the parameters of the kinetic models. The linear regression of experimental data according to Eq. (12) is reported in Fig. 3A and k_1 resulted 0.143 min^{-1}. The comparison of the regression and the experimental data suggests that the model can be successfully adopted to describe the adsorption dynamic far from equilibrium conditions, within the first 10 min. In other words, the pseudo-first order model may be adopted provided that

equation(17)

$$\frac{\langle q \rangle(t)}{\langle q_{eq} \rangle} < \theta_1$$ ⟨q⟩ (t) ⟨qeq⟩ <θ1

where ϑ_1 marks the fraction of biosorbent saturation above which the expected adsorbed dye concentration departs from the experimental value. With reference to Fig. 3A, ϑ_1 resulted 0.83.

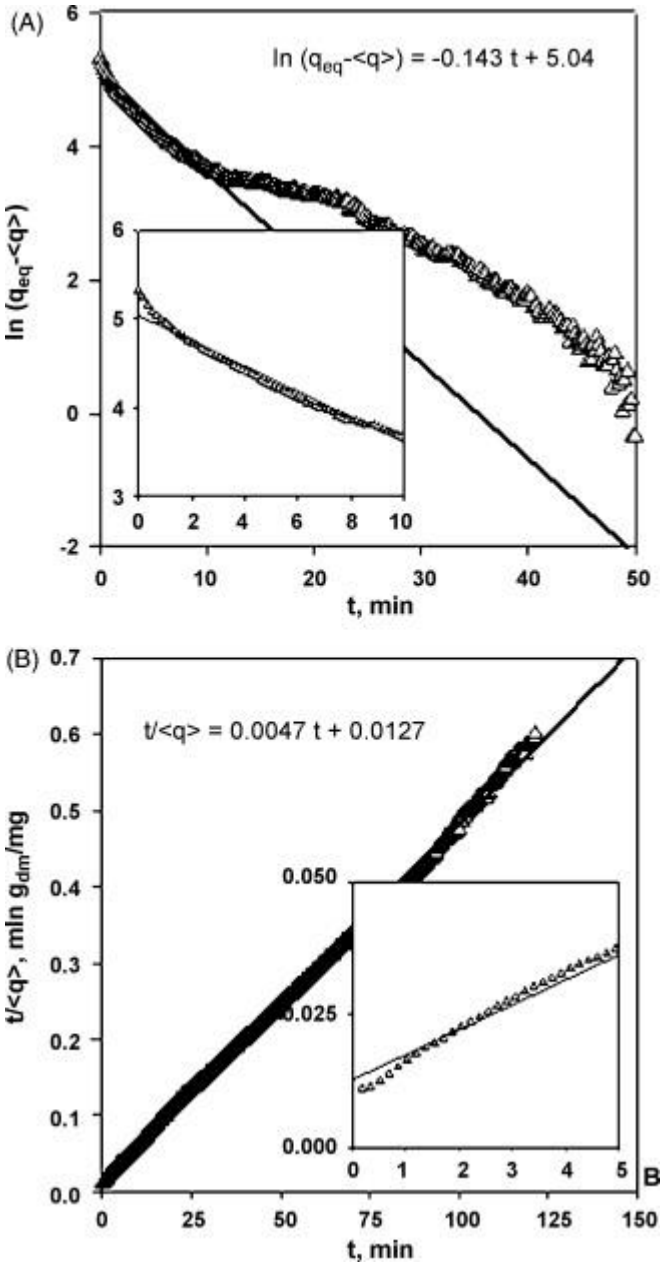

Fig. 3. Regressions of experimental data (t, $\langle q \rangle$) reported in Fig. 2 in agreement with: (A) Eq. (12) and (B) Eq. (13).

The best fitting of the time-series ($t/\langle q \rangle$) versus t according to Eq. (13) is reported in Fig. 3B. The parameter k_2 resulted 0.0019 $g_{DM}/(g_{dye}$ min). The comparison of the model with experimental data suggests that the model can be successfully adopted to describe the adsorption dynamic except for the beginning of the process. Accordingly, the pseudo-second order model satisfactorily describes the experimental data in the interval:

equation(18)

$$\theta_2 < \frac{\langle q \rangle(t)}{\langle q_{eq} \rangle} < 1$$

θ2< ⟨q⟩ (t) ⟨qeq⟩ <1

where ϑ_2 marks the fraction of biosorbent saturation below which the expected value of dye uptake Eq. (18) considerably deviates from the experimental data. With reference to Fig. 3B, ϑ_2 resulted 0.81.

It is interesting to note that the intervals of reliability of the models expressed in terms of the ratio $\langle q \rangle$ / $\langle q_{eq} \rangle$ overlap: θ_2 is smaller than θ_1. This condition allows to describe the biosorption process with continuity from the beginning of the test up to the equilibrium.

Biosorption tests carried out with dye solutions of AR266 at initial concentration ranging between 90 and 250 mg_{dye}/L confirm the dynamics reported in Fig. 2. Results of linear regression of data according to Eqs. (12) and (13) for selected tests are reported in Table 1, together with the values of θ_1 and θ_2. The table also reports the results of selected tests carried out with dye solutions of ABu62 and AY49 at initial concentration ranging between 90 and 520. Eventually, also the averaged values of the model parameters and of θ_1 and θ_2 are reported.

Table 1. Parameters of the kinetics model of a representative set of tests. Mono-dye solutions.

Dye	c_T^0, mg_{dye}/L	k_1, min^{-1}	ϑ_1	k_2, $g_{DM}/(mg_{dye}min)$	ϑ_2
AR266	95	0.015	0.64	0.0001	0.32
	170	0.022	0.78	0.0019	0.53
	230	0.090	0.88	0.0007	0.83
	250	0.143	0.83	0.0019	0.81
	Mean[a]	0.058	0.78	0.0012	0.59
ABu62	180	0.22	0.89	0.003	0.90
	230	0.27	0.88	0.01	0.92
	350	0.10	0.85	0.001	0.70
	450	0.04	0.89	0.001	0.76
	520	0.31	0.91	0.002	0.52
	Mean[a]	0.22	0.88	0.0034	0.85
AY49	100	0.18	0.92	0.009	0.04
	190	0.17	0.87	0.005	0.75
	280	0.11	0.88	0.002	0.05
	340	0.05	0.95	0.001	0.02
	410	0.07	0.86	0.015	0.73
	Mean[a]	0.13	0.9	0.0064	0.32

a Value estimated on all tests carried out.

The analysis of model parameters in Table 1 suggests that: (i) there is no effect of the initial concentration of the dye on both the kinetic parameters and the characteristic ratios θ_1 and θ_2; (ii) the coexistence of both models (i.e. $\theta_2 \leq \theta_1$) applies for almost all operating conditions tested. Furthermore, the low values of θ_2 highlight that the pseudo-second order model could be safely adopted in a large interval of the adsorption process.

Fig. 4 shows experimental data regarding a biosorption test carried out with the model wastewater at initial total dye concentration of 150 mg/L (MW150). The time-series of each dye concentration on the sorbent and the total dye uptake have been reported. It is noteworthy that the concentration of AY49 and of ABu62 are characterized by a maximum, particularly marked for ABu62. This behaviour suggests the occurrence of competitive dye adsorption phenomena: all the three dyes are adsorbed at higher rates at the beginning of the process, but once the fraction of free active sites diminishes the competition among dyes appears [20]. In the reported test, further adsorption of AR266 was coupled with partial desorption of both ABu62 and AY49, therefore the biomass showed higher selectivity towards the red dye. The analysis of the time-series of each dye concentration in agreement with the kinetic models (Eqs. (12) and (13)) provided the parameters k_1, k_2, θ_1 and θ_2 for the MW reported in Table 2.

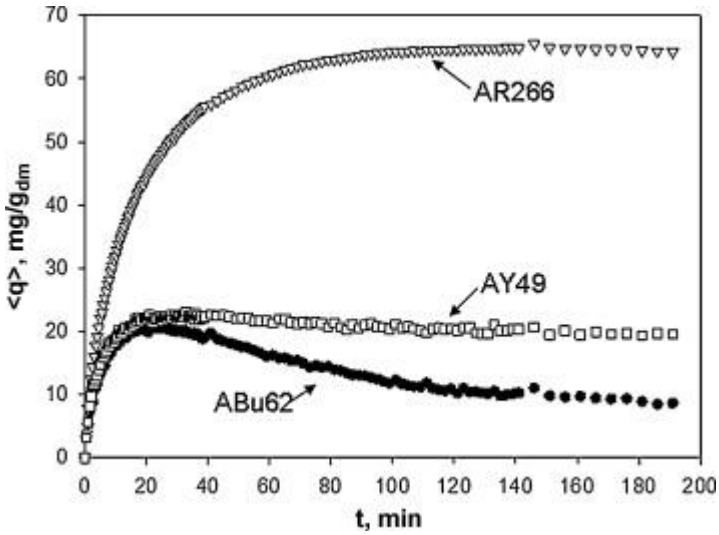

Fig. 4. Time-resolved concentration of dyes on *C. elegans*. Liquid volume: 0.1 L; biomass: 0.03 g; c_T^0 = 150 mg/L.

Table 2. Parameters of the kinetics model of a representative set of tests. Model wastewater.

Dye	Model wastewater	c_T^0[a], mg_{dye}/L	k_1, min^{-1}	ϑ_1	k_2, g_{DM}/mg_{dye} min	ϑ_2
AR266	MW60	65	0.04	0.86	0.0192	0.33
	MW150	123	0.038	0.96	0.0011	0.29
	MW350	360	0.18	0.42	0.0008	0.64
		Mean	0.086	0.75	0.007	0.42
ABu62	MW60	65	0.19	0.85	0.03	0.62
	MW150	123	0.93	0.93	0.061	1.46
	MW350	360	1.06	0.9	0.005	1.3
		Mean	0.73	0.89	0.032	1.13
AY49	MW60	65	0.21	0.86	0.065	0.66
	MW150	123	0.17	0.9	0.025	0.75
	MW350	360	0.45	0.75	0.210	0.94
		Mean	0.28	0.84	0.10	0.78

a

The mass ratio among the dyes was 1:1:1.

Tests carried out with the MW at nominal total dye concentration 60 and 350 mg/L confirmed the behaviour observed in Fig. 5. Table 2 reports the value of the kinetic parameters and of θ_1 and θ_2. The parameters k_1 and k_2 are higher than the values assessed for single dye biosorption tests. The overlapping of the pseudo-first and the pseudo-second order models is still recognized ($\theta_2 \leq \theta_1$), except for the most concentrated MW. It is noteworthy that ABu62 is characterized by θ_2 larger than 1 because the curve (t,q) shows a maximum larger than the equilibrium value q_{eq} (see Fig. 4).

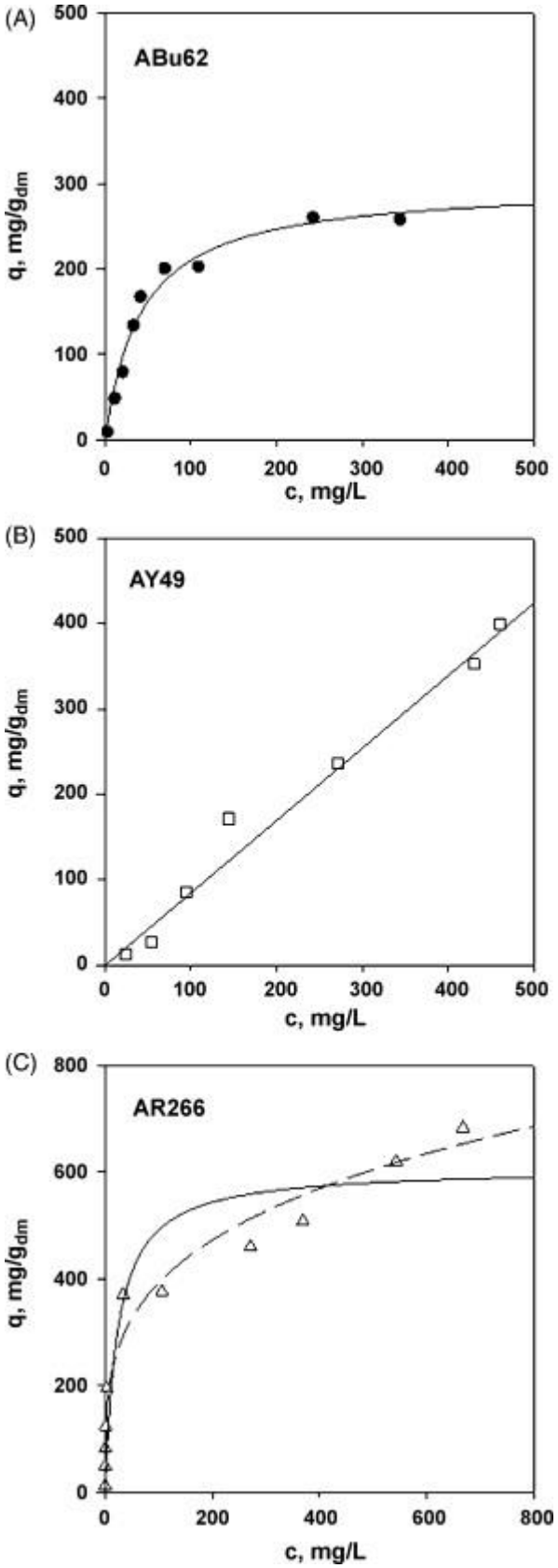

Fig. 5. Equilibrium data of biosorption of single acid dyes. ABu62: solid line—Langmuir isotherm (Eq. (14)). AY49: solid line—linear isotherm (Eq. (15)). AR266: solid line—Langmuir isotherm (Eq. (14)); dashed line—Freundlich isotherm (Eq. (16)).

At the best of our knowledge, the presented results concerning biosorption kinetics cannot be safely compared to those available in the literature due to the different operating conditions applied (e.g. Vijayaraghavan et al. [21]).

4.2. Assessment of biosorption equilibrium

The equilibrium data of biosorption of the dyes on *C. elegans* lyophilised biomass are reported in Fig. 5. The pH at the beginning of tests was set at 5 as described in Section 2.1, and at the end of the tests increased up to 6–7. Present investigation coupled with tests concerning the biosorption of the MW on lyophylised biomass up to saturation (Table 3) showed that the biosorption capacity is almost constant provided that the equilibrium pH ranges between 6 and 7. Therefore, the data of equilibrium measured under the operating conditions adopted in the present study do not depend on the pH and may be worked out accordingly to the models reported in Section 3.2. Furthermore, the adsorption isotherms confirm that the AR266 is characterized by the largest affinity towards *C. elegans* biomass. The biosorption of ABu62 on *C. elegans* was successfully described by the Langmuir model (Eq. (14)) and it is characterized by a maximum adsorption capacity of about 300 mg_{dye}/g_{DM}. The biosorption of AY49 was linear with the dye concentration in the liquid phase and characterized by a repartition coefficient 0.848 L/g_{DM}. The Freundlich model (Eq. (16)) successfully describes the equilibrium data of AR266. Parameters of the equilibrium models were assessed for each dye and are reported in Table 4.

Table 3. Maximum biosorption capacity as a function of the initial pH for the model wastewater, after Tigini et al. [22].

Initial pH	3	5	7	9	11
Average pH at the equilibrium	3	6.4	7.1	7.3	10
Maximum adsorption capacity, mg_{dye}/g_{DM}	1035 ± 17	824 ± 23	930 ± 91	945 ± 104	667 ± 67

Table 4. Parameters of the equilibrium models reported in Section 3.2.

	Q_{max}, mg_{dye}/g_{DM}	K_L, L/mg_{dye}	K, L/g_{DM}	n	K_F $(mg_{dye}^{(n-1)}L)^{1/n}/g_{DM}$
ABu62	300	0.024	–	–	–
AR266	610	0.043	–	3.7	114
AY49	–	–	0.848	–	–
MW	420	0.006	–	2.2	19

Fig. 6 details the equilibrium data referred to each dye measured during the equilibrium tests carried out with the MW. The total dye concentration at equilibrium in the liquid and in the sorbent phases is also reported in Fig. 6 and has been worked out in agreement with both the Langmuir and the Freundlich models. The parameter models referred to the total dye concentration are reported in Table 4. The analysis of the equilibrium data shows that *C. elegans* biomass is characterized by a remarkable decrease in the biosorption capacity with reference to both ABu26 and AY49, when compared with single dye solutions. On the other hand, biosorption capacity of AR266 appears to

be less affected by the presence of the other two dyes, mirroring the same results observed for the adsorption kinetic studies.

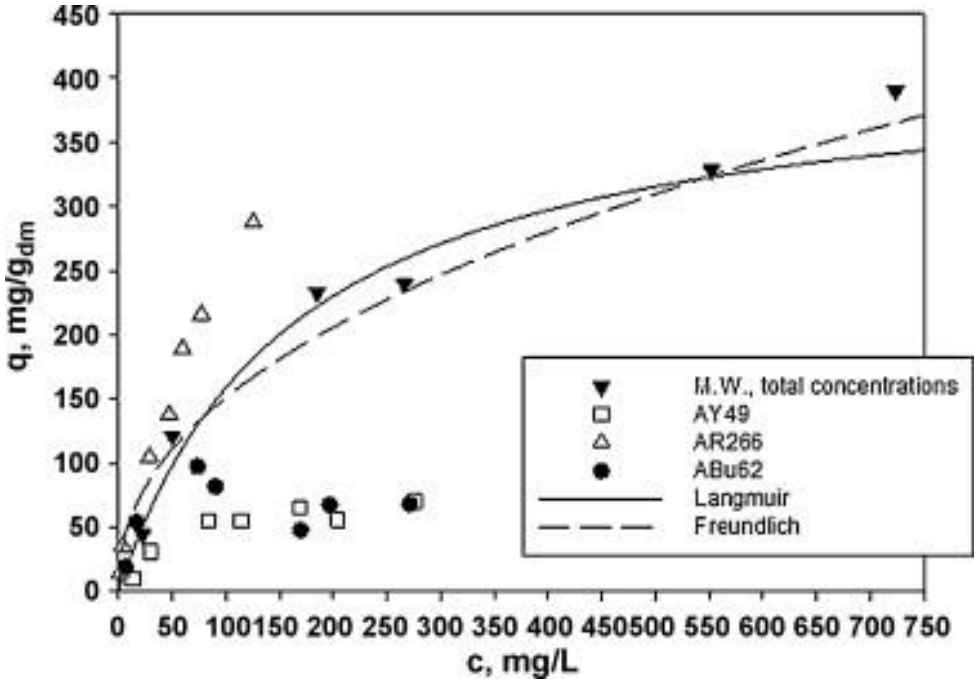

Fig. 6. Equilibrium data of simultaneous biosorption of three acid dyes.

The different biosorption affinity/capacity of the *C. elegans* with respect to the three dyes may be interpreted taking into account several factors, including pH, ionic strength, dye features (molecular weight, characteristics of the main functional groups, molecular structure), simultaneous presence of different dyes and their concentration [6] and [12].

4.2.1. Temperature, salt concentration, pH

Tests have been carried out setting temperature, salt concentration and initial pH at fixed values. Furthermore, the small increase of the equilibrium pH with respect to the initial pH does not affect significantly the biomass adsorption capacity. As a consequence, the different behaviour observed during tests cannot be ascribed to any of these factors, but rather to specific features of the investigated dye.

4.2.2. Dye features

The molecular weight of the three dyes is quite close each other. The molecule charges are comparable and there is a sulphonic group – responsible of the salt formation – and an ammine group for each dye. Therefore, the different affinity of the biomass towards the dyes is not due to these features, as suggested by Maghami and Roberts [23]. Anyway, the functional groups specific of each dye (Fig. 1) can be considered responsible for the different adsorption capacities of the biomass towards each dye as well as for the marked selectivity towards AR226. In particular, the $-CF_3$ functional group characterized by a high negative charge density that may allow a suitable interactions with the $-NH_x$ active sites of the biomass.

Interesting results may be pointed out when comparing the *C. elegans* affinity/capacity towards the dyes investigated with data available in the literature: the maximum adsorption capacity is definitively higher than the value reported in previous investigations. As an example, Kiran et al.

[24] reported that *Cephalosporium aphidicola* was characterized by q_{max} = 109 mg_{dye}/g_{DM} towards AR57. *Aspergillus niger*, *Phellinus ignarius*, *Fomes fomentarius* and *Rhizopus stolonifer* were characterized by q_{max} as large as 230 mg_{dye}/g_{DM} towards Congo red, Methylene blue, Rodhamina B and Bromophenol blue [25]. Similarly, the occurrence of strong mutual interferences between acid dyes during adsorption tests is observed according with previous results reported in the literature [6], [7], [12], [13] and [26].

5. Conclusions

Acid dye – Acid Blue 62, Acid Red 266, Acid Yellow 49 – in mono-dye solutions and in multi-dye solutions have been successfully adsorbed on lyophilised biomass of *C. elegans*. Kinetic rates and equilibrium conditions of the biosorption have been characterized.

The kinetic characterization has been carried out paying attention at the assessment of the intrinsic adsorption rates, a key phenomenon in the design and optimization of the adsorption unit regardless typology of two-phase contact technology (agitated vessel, fixed bed columns, fluidized bed columns, etc.). Experimental apparatus and procedures have been purposely developed for the assessment of the biosorption kinetic. The system aimed to control the fluid–particle mass transfer rate and, in particular, the apparatus was operated under operating conditions characterized by external mass transfer rate negligible with respect to the intraparticle adsorption rates. Accordingly, reliable intraparticle biosorption kinetics may be determined and it may be adopted as a soundness tool to compare different sorbents. The intraparticle kinetics coupled with external mass transfer relationships – available for the different typologies of two-phase contact systems – allow to design, control and optimize bioadsorption units.

The adsorption capacity of *C. elegans* versus the investigated dyes resulted larger than capacities reported in the literature and recently reviewed by Aksu [12]. Both kinetics and equilibrium tests confirm that the biomass is more selective towards AR266, probably for the high negative charge density of the $–CF_3$ functional that may easily interact with the $–NH_x$ active sites of the biomass.

The adsorption kinetic was described by means of a pseudo-first order model and a pseudo-second order model. The first is valid for far-from-saturation conditions, i.e. at the beginning of biosorption on virgin biomass. The pseudo-second order kinetic model can be successfully adopted to describe the biosorption process over a wider time interval, close to the equilibrium conditions.

Biosorption tests carried out with multi-dye solutions highlight that the adsorption capacity of the biomass decreases and the kinetics increased when compared with data assessed for single dye solution tests. As a consequence, the design of biosorption units based on single-dye investigation may lead to unreliable results data. The effects of the interaction between dye-molecules on the biosorption process need to be further investigated.

Even though reliable guidelines for the design, control and optimization of an adsorber for dye removal with biomasses of *C. elegans* is far from being accomplished, a preliminary estimation of the characteristic time scale of the biosorption process can be obtained from the kinetic parameters assessed in the present study. According to the pseudo-first order model, the reciprocal of k_1 yields the time scale of the adsorption process. In particular, for all the dyes the reciprocal of k_1 ranges between few minute and a dozens of minute. According to the pseudo-second order model, the characteristic time scale may be assessed as the reciprocal of the product $k_2 q_{ref}$, where q_{ref} is the adsorbed dye concentration in the outlet stream. Assuming an average value of k_2 and $O(q_{ref}) = 10^2$ mg_{dye}/g_{DM}, the characteristic time scale of the biosorption process still ranges between

1 and 10 min. As a rule of thumb, the space-time of the adsorption unit for the system investigated results to be of the order of a dozen of minutes.

Acknowledgements

The Authors are indebted with Mrs Mariella Cecere and Mrs Irene Grosso for their assistance in experimental investigation. The research was funded by Compagnia di San Paolo (Progetto BIOFORM) and by Marcopolo Environmental Group.

References

[1] N. Mathur, P. Bhatnagar Mutagenicity assessment of textile dyes from Sanganer (Rajasthan) J. Environ. Biol., 28 (2007), pp. 123–126

[2] G. Crini Non-conventional low-cost adsorbents for dye removal: a review Bioresour. Technol., 97 (2006), pp. 1061–1085

[3] F.I. Hai, K. Yamamoto, K. Fukushi Hybrid treatment system for dye wastewater Crit. Rev. Environ. Sci. Technol., 37 (2007), pp. 315–377

[4] T. Robinson, G. McMullan, R. Marchant, P. Nigam Remediation of dyes in textile effluent: a critical review on current treatment technologies with a proposed alternative Bioresour. Technol., 77 (2001), pp. 247–255

[5] O. Olivieri, A. Di Donato, A. Marzocchella, P. Salatino Bioreactors for azo-dye conversion A.H. Erkurt (Ed.), Biodegradation of Azo Dyes: The Handbook of Environmental Chemistry, vol. 9, Springer-Verlag, Berlin Heidelberg (2010), pp. 101–131

[6] G.M. Gadd Biosorption: critical review of scientific rationale, environmental importance and significance for pollution treatment J. Chem. Technol. Biotechnol. (2008) doi 101002/jctb.1999

[7] M.S. Chiou, P.Y. Ho, H.Y. Li Adsorption behavior of dye AAVN and RB4 in acid solutions on chemically crosslinked chitosan beads J. Chin. Inst. Chem. Eng., 34 (2003), pp. 625–634

[8] A.R. Cestari, E.F.S. Vieira, A.A. Pinto, E.C.N. Lopes Multiple adsorption of anionic dyes on silica/chitosan hybrid. 1. Comparative kinetic data from liquid- and solid-phase models J. Colloid. Int. Sci., 292 (2005), pp. 363–372

[9] M.S. Chiou, G.S. Chuang Competitive adsorption of dye metanil yellow and RB15 in acid solutions on chemically cross-linked chitosan beads Chemosphere, 62 (2006), pp. 731–740

[10] V. Prigione, G.C. Varese, L. Casieri, V.F. Marchisio Biosorption of simulated dyed effluents by inactivated fungal biomasses Bioresour. Technol., 99 (2008), pp. 3559–3567

[11] V. Prigione, V. Tigini, C. Pezzella, A. Anastasi, G. Sannia, G.C. Varese Decolorisation and detoxification of textile effluents by fungal biosorption Water Res., 42 (2008) 2911-2920 b

[12] Z. Aksu Application of biosorption for the removal of organic pollutants: a review Process Biochem., 40 (2005), pp. 997–1026

[13] G. Crini, P.M. Badot Application of chitosan, a natural aminopolysaccharide, for dye removal from aqueous solution by adsorption process using batch studies: a review of recent literature Prog. Polym. Sci., 33 (2008), pp. 399–447

[14] K. Vijayaraghavan, Y.-S. Yun Bacterial biosorbents and biosorption Biotechnol. Adv., 26 (2008), pp. 266–291

[15] V. Prigione, M. Zerlottin, D. Refosco, V. Tigini, A. Anastasi, G.C. Varese Chromium removal from a real tanning effluent by autochthonous and allochthonous fungi Bioresour. Technol., 100 (2009), pp. 2770–2776

[16] V. Prigione, G.C. Varese, L. Casieri, S. Voyron, A. Bertolotto, V. Filipello Marchisio Use of Cunninghamella elegans Lendner in Methods for Treating Industrial Wastewaters Containing Dyes (2007) Patent number EP07118877.5

[17] E.J. Wilson, C.J. Geankoplis Liquid mass transfer at very low Reynolds numbers in packed beds Ind. Eng. Chem. Fundam., 5 (1966), pp. 9–14

[18] T. Kataoka, H. Yoshida, K. Ueyama Mass transfer in laminar region between liquid and packing material surface in the packed bed J. Chem. Eng. Jpn., 5 (1972), p. 132

[19] Y.S. Ho, G. McKay Pseudo-second order model for sorption processes Process Biochem., 34 (1999), pp. 451–465

[20] D.M. Ruthven Principles of Adsorption & Adsorption Process J. Wiley & Sons, New York (1984)

[21] K. Vijayaraghavan, M.W. Lee, Y.-S. Yun A new approach to study the decolourization of complex reactive dye bath effluent by biosorption technique Biores. Technol., 99 (2008), pp. 5778–5785

[22] V. Tigini, I. Donelli, V. Prigione, F. Di Natale, M.E. Russo, G. Freddi, A. Marzocchella, G.C. Varese Cunninghamella elegans biomass, an innovative biosorbent material towards different organic and inorganic pollutants Proc. 6th International Conference on Textile and Polymer Biotechnology, 9789081392419 (2009)

[23] G.G. Maghami, G.A. Roberts Studies of the interaction of anionic dyes on chitosan Macromol. Chem. Phys., 189 (1988), pp. 2239–2243

[24] I. Kiran, T. Akar, A.S. Ozcan, A. Ozcan, S. Tunali Biosorption kinetics and isotherm studies of Acid Red 57 by dried *Cephalosporium aphidicola* cells from aqueous solution Biochem. Eng. J., 31 (2006), pp. 197–203

[25] P. Kaushik, A. Malik Fungal dye decolourization: recent advances and future potential Environ. Int., 35 (2009), pp. 127–141

[26] M.S. Chiou, H.Y. Li Adsorption behavior of reactive dye in aqueous solution on chemical cross-linked chitosan beads Chemosphere, 50 (2003), pp. 1095–1105